Original Paper

Eletrônica de Potência
Open Journal of Power Electronics



Received August 24, 2026; Received in revised form October 20, 2026; Accepted November 12, 2026; Date of publication November 25, 2026.
The review of this paper was arranged by Associate Editor Pedro J. dos S. Neto and Editor-in-Chief Allan F. Cupertino.
Digital Object Identifier http://doi.org/10.18618/REP.e202644

Development and Experimental Evaluation of an Integrated Virtual Instrumentation System for Arc Flash Incident Energy Measurement

Andrey A. S. Pereira[1,*], Pedro O. Bacin[1], Vitor C. Bender[1], Marcio Bottaro[2], Tiago B. Marchesan[1], Gilnei J. G. dos Santos[3], Jéssica P. Begossi[3]

[1]Federal University of Santa Maria (UFSM), Institute of Energy and Mobility (IEM), Santa Maria, RS, Brazil.
[2]University of São Paulo (USP), Institute of Energy and Environment (IEE), São Paulo, SP, Brazil.
[3]CPFL Energia, Campinas, SP, Brazil.

e-mail: andrey.pereira@acad.ufsm.br*; pedro.bacin@acad.ufsm.br; vitor.bender@ufsm.br; marcio@iee.usp.br; tiago@ufsm.br; gilnei.santos@cpfl.com.br; jessica.begossi@cpfl.com.br.
*Corresponding author.

ABSTRACT Experimental determination of incident energy (IE) in arc flash testing requires integrating calorimetry, signal acquisition, and thermal processing; when performed separately, these tasks may increase operator intervention and hinder data-flow standardization. This study developed and experimentally evaluated an integrated system for IE measurement in arc flash tests. The architecture combines copper calorimeters instrumented with Type K thermocouples and arranged according to the spatial configuration adopted in the IEEE Std 1584-2018 test program, galvanically isolated data acquisition, and a LabVIEW®-based virtual instrument (VI) for monitoring, thermal-parameter identification, Shomate-based enthalpy calculations, and data storage. The calorimeters satisfied the functional-verification criterion of IEC 61482-1-1, and the VI-based IE calculation showed numerical agreement with an independently implemented reference calculation. Across 18 tests, comprising 10 tests with vertical electrodes in open air (VOA) and 8 with horizontal electrodes in open air (HOA), measured IE remained below the corresponding IEEE Std 1584-2018 estimates, with relative differences from -29.3% to -2.6% and a mean of -12.7%. This ordering was consistent under the evaluated conditions, although the magnitude of the difference varied among tests and should not be generalized beyond the investigated experimental set. The proposed integration consolidates calorimetric IE acquisition, processing, and comparison into a single workflow.

KEYWORDS Arc flash, IEEE 1584, Incident energy, Temperature measurement, Virtual instrumentation.

An arc flash consists of a sustained electrical discharge through an ionized gaseous medium, accompanied by the emission of electromagnetic radiation and the intense release of thermal energy [1]. In electrical systems, this phenomenon represents one of the most severe occupational hazards, since the temperatures developed may reach values on the order of 20,000 K, particularly near the electrodes [2]. The associated thermal exposure is commonly quantified in terms of incident energy (IE), defined as the thermal energy per unit area received by a surface at a specified distance from the arc source [3]. Determining IE is an important step in arc flash hazard assessment and provides a basis for selecting personal protective equipment (PPE) consistent with the safety requirements established by NFPA 70E® [4].

In Brazil, the importance of IE assessment was reinforced by Ordinance MTE No. 737/2026, which approved the revised Brazilian Regulatory Standard number 10 (NR-10). The new text addresses exposure to electric arcs and requires electrical designs, when applicable, to consider an IE study for protection against the thermal effects of arc flash. It also uses IE to establish safe working distances and select PPE when the conditions specified in the regulation do not apply [5]. These requirements reinforce the need for reliable IE assessment methods and measurement systems.

To estimate IE in arc flash scenarios, IEEE Std 1584-2018 provides empirical models developed from approximately 1,800 three-phase arc flash tests, covering systems with voltages ranging from 208 V to 15 kV. Although these models account for relevant electrical parameters and equipment construction characteristics, arc behavior and the energy transferred to the surroundings remain sensitive to electrode geometry, arc configuration, and specific exposure conditions [3]. In this context, experimental measurements are necessary to characterize thermal exposure under different configurations and laboratory conditions, assess the performance of measurement systems, and support comparison with IEEE Std 1584-2018 estimates.

Experimental IE measurement typically relies on copper-disk calorimeters instrumented with thermocouples and mounted in thermally insulating supports, following ASTM

CC BY

F1959/F1959M and IEC 61482-1-1 [6]–[8]. Measurement performance depends on the design of the calorimetric assembly and the signal-acquisition architecture. The calorimeter geometry and insulation materials affect its thermal response and transient behavior [9], while junction integrity and thermal coupling between the thermocouple and the copper disk are essential for representing the temperature of the energy-absorbing element [10], [11]. In high-power laboratories, the low-level thermocouple signals are also susceptible to electromagnetic interference (EMI) generated by high currents and voltage transients, which must be considered in the acquisition-system design [12], [13].

In addition to the physical aspects of the instrumentation, IE determination requires processing the temperature curves, selecting the initial and maximum temperatures, and converting the measured temperature rise into absorbed energy. The Shomate equation, together with the NIST thermochemical coefficients for solid copper, enables the enthalpy change to be determined over the recorded range [14].. However, when signal acquisition, thermal-parameter identification, and IE calculation are performed as separate steps, the processing becomes more dependent on operator intervention and hinders the standardization of the data flow. Integrating these functions into a virtual instrumentation environment can reduce non-integrated post-processing steps, organize the data flow, and improve processing traceability [15].

In this context, this study develops and experimentally evaluates an integrated system for IE measurement in arc flash tests. Implemented at the High Current Laboratory (HCLab) of the Federal University of Santa Maria (UFSM), the system combines seven copper calorimeters instrumented with Type K thermocouples and arranged according to the spatial configuration adopted in the IEEE Std 1584-2018 test program, a galvanically isolated data-acquisition interface, and a VI developed in LabVIEW®. The system integrates temperature acquisition, thermal-parameter identification, Shomate-based enthalpy calculations, automated IE determination, visualization, and structured data storage. Its experimental evaluation includes functional verification of the calorimeters, analysis of a selected three-phase test with vertical electrodes in open air, numerical verification of the IE calculation, and comparison of calorimetric measurements with IEEE Std 1584-2018 calculations across an expanded set of 18 tests with vertical electrodes in open air (VOA) and horizontal electrodes in open air (HOA) under varying electrical and geometric conditions.

An earlier version of this study, presented at SEPOC 2025, focused on the development of the calorimetric instrumentation, functional verification of the sensors, and IE determination in a selected arc flash test [16]. The present article extends that work through a dedicated VI, automated thermochemical processing, a more detailed analysis of the selected test, numerical verification of the calculation procedure, and an expanded experimental data set comprising 10 VOA and 8 HOA tests. The extended data set also enables a quantitative comparison between the measured IE values and the corresponding IEEE Std 1584-2018 estimates over different test conditions.

I. EXPERIMENTAL SETUP AND CALORIMETRIC INSTRUMENTATION

This section presents the experimental infrastructure, calorimetric instrumentation, sensor arrangement, and test conditions used in the arc flash experiments. Controlled arc generation and thermocouple-based copper calorimetry are combined to quantify the resulting thermal exposure.

A. High-Current Laboratory and Arc Flash Generation

The arc flash tests were conducted at HCLab, UFSM. The laboratory infrastructure includes a 5 MVA three-phase transformer, adjustable single-phase reactors for controlling the prospective short-circuit current, and circuit breakers operated by digital protection relays. The facility was designed to support three-phase arc flash tests with prospective short-circuit currents ranging from 1 kA to 20 kA [17]. The test facility layout is shown in Fig. 1.

The facility is divided into three functional areas: the high-power circuit, the test chamber, and the measurement area. The transformer supplies the electrode system through current-limiting reactors and switching and protection devices. The electrodes and calorimeter support are installed inside the test chamber, whereas the measurement system remains outside the direct arc-exposure region. The arc is initiated by a fuse wire placed between the electrodes, and its duration is controlled by digital protection relays acting on the circuit breakers. This arrangement allows the prospective current, arc duration, electrode geometry, and working distance to be defined for each test.

B. Calorimeter Design and Thermocouple Attachment

The IE measurement system comprises seven calorimeters made of electrolytic-copper disks instrumented with Type K thermocouples. Each disk has a mass of approximately 18 g, a diameter of 40 mm, and a thickness of 1.6 mm. The exposed surface is coated with a thin layer of matte black paint, and the disk is mounted in a Marinite A® support for thermal and electrical insulation, as shown in Fig. 2 [7], [18]. Marinite A® was selected because of its availability in South America, particularly in Brazil. Although IEC 61482-1-1 recommends Marinite P®, I&M®, and Monolux® 500, previous tests showed that Marinite A provided comparable thermal performance, without relevant effects on the measured temperatures or IE estimates [9]. It was therefore adopted as a practical alternative for the proposed calorimeter design.

The calorimeter is treated as a coupled thermal system in which the copper disk acts as the energy-absorbing element, while the insulating support limits heat transfer to the surrounding structure. Therefore, the geometry and constituent materials of the calorimetric assembly influence its thermal

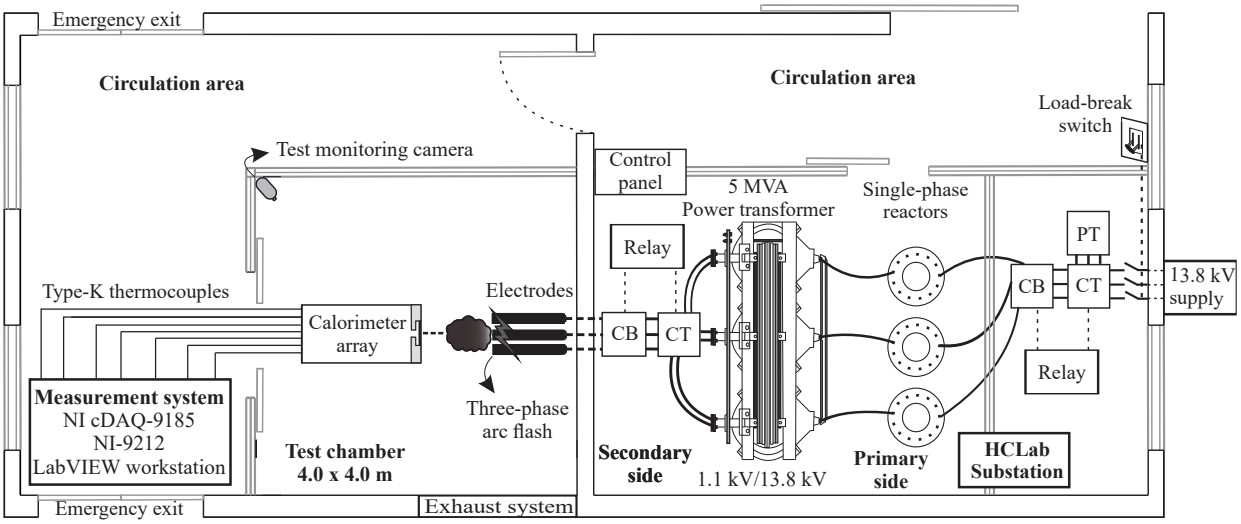


FIGURE 1. Layout of the substation and arc flash test infrastructure at the High Current Laboratory (HCLab) [19].

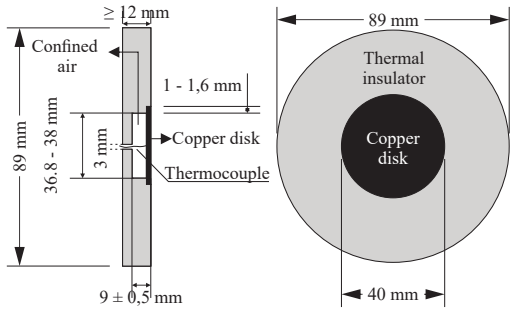


FIGURE 2. Geometry and dimensions of the copper disk calorimeter.

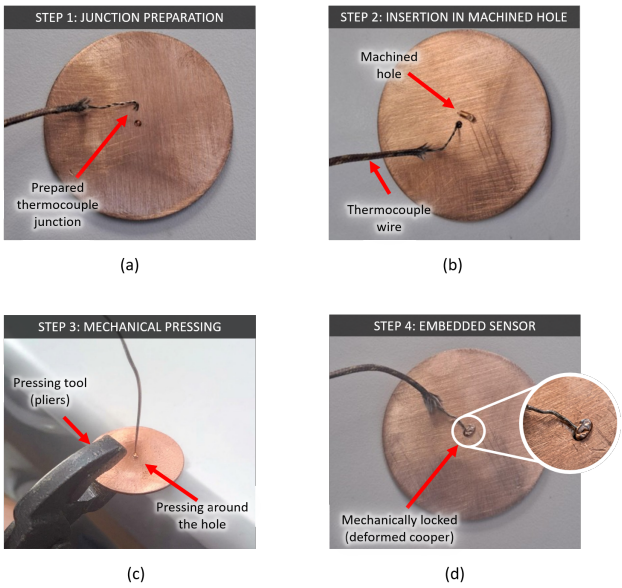


FIGURE 3. Thermocouple attachment procedure: (a) junction preparation; (b) insertion into the machined hole; (c) mechanical pressing; and (d) disk after thermocouple attachment.

inertia and transient response [9], [20]. These characteristics must be considered when relating the measured temperature rise to the energy absorbed by the sensor.

The measured thermal response also depends on the mechanical and thermal coupling between the thermocouple junction and the copper disk. In the proposed assembly, the thermocouple is inserted into a machined hole on the rear surface of the disk and mechanically attached through a pressing procedure, as illustrated in Fig. 3. This technique establishes direct contact between the thermocouple junction and the energy-absorbing element without introducing welding or filler materials into the measurement region, following the thermocouple-based calorimetric approach adopted in ASTM F1959/F1959M and IEC 61482-1-1 [6], [7].

C. Calorimeter Arrangement and Test Geometry

The seven calorimeters were mounted on a common support according to the spatial arrangement adopted in the IEEE Std 1584-2018 test program [3]. The central calorimeter was aligned with the electrode tips, and the other six were distributed around it. The center-to-center spacing between adjacent calorimeters was 152.4 mm.

For the selected VOA test analyzed in detail in this study, the calorimeter plane was positioned at a working distance of 500 mm, measured from the electrode tips to the exposed surfaces of the copper disks. The test used three vertical electrodes with a 100 mm gap. Additional HOA and VOA tests included in the comparative analysis were performed under different electrical and geometric conditions.

This arrangement enabled simultaneous IE measurements at the central and surrounding positions, providing a spatial characterization of the thermal exposure. Figure 4 shows the overall experimental arrangement and the calorimeter numbering from the rear data-acquisition side. The acquisition components are described in the following section.

CC BY

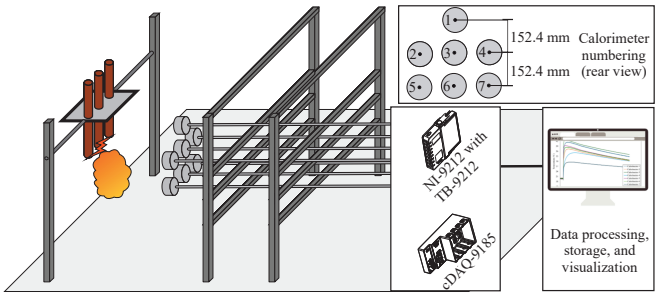


FIGURE 4. Experimental setup for thermocouple-based IE measurements.

D. Support Structure and Positioning

To ensure reproducible calorimeter positioning and mechanical stability during arc flash tests, a modular support structure was developed, as shown in Fig. 5(a). The main frame was assembled using T-slot extruded aluminum profiles, allowing the calorimeter arrangement to be adjusted according to the required test geometry.

Each calorimeter was mounted on an individual holder machined from 1020 carbon steel, detailed in Fig. 5(b). The holder provides mechanical fixation of the calorimeter and connection to the protective cable routing. To reduce EMI and protect the thermocouple wiring from mechanical stress, the cables were routed through rigid 1/2-inch galvanized-steel tubes connected to the rear of the holders and subsequently through flexible stainless-steel conduits.

II. DATA ACQUISITION AND PROCESSING SYSTEM

The proposed system integrates isolated thermocouple signal acquisition, automated thermal-curve processing, IE calculation, visualization, and structured data storage within a LabVIEW-based architecture. This section describes the acquisition hardware and EMI-mitigation measures, the architecture and operational workflow of the developed virtual instrument (VI), and the computational procedure used to determine and store the IE values.

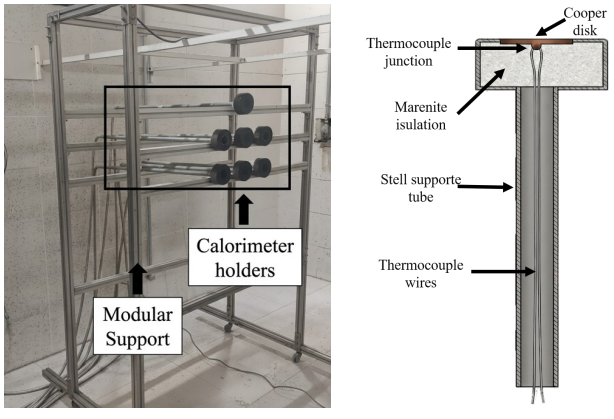


FIGURE 5. Experimental support structure and calorimeter positioning: (a) overall arrangement and (b) calorimeter support detail.

A. Acquisition Architecture and VI Workflow

The Type K thermocouples attached to the seven calorimeters were connected to NI-9212 modules installed in an NI cDAQ-9185 chassis. The acquisition system was configured to operate at a sampling rate of 95 S/s and provided channel-to-channel galvanic isolation of up to 250 V_{rms}. The acquisition hardware and signal path are identified in the overall experimental arrangement shown in Fig. 4.

Arc flash tests involve high currents and rapid voltage transients that may affect the low-level signals generated by thermocouples. To reduce susceptibility to EMI and ground-loop effects, the acquisition architecture combined galvanic isolation with dedicated grounding, shielded cables, and appropriate separation and routing of the signal cables. These measures were adopted to maintain stable and continuous temperature records during the tests [12].

The acquisition hardware was integrated with a VI developed in LabVIEW for signal acquisition, monitoring, visualization, processing, and storage. Similar virtual-instrumentation architectures have been employed to integrate measurement hardware with automated signal-processing routines in experimental electrical systems [21]–[23]. The operational workflow of the developed system is presented in Fig. 6.

The VI coordinates the configuration of the measurement channels, continuous acquisition of the calorimeter temperatures, real-time visualization of the thermal curves, and transfer of the recorded data to the IE calculation routine. The acquisition loop remains active until it is stopped by

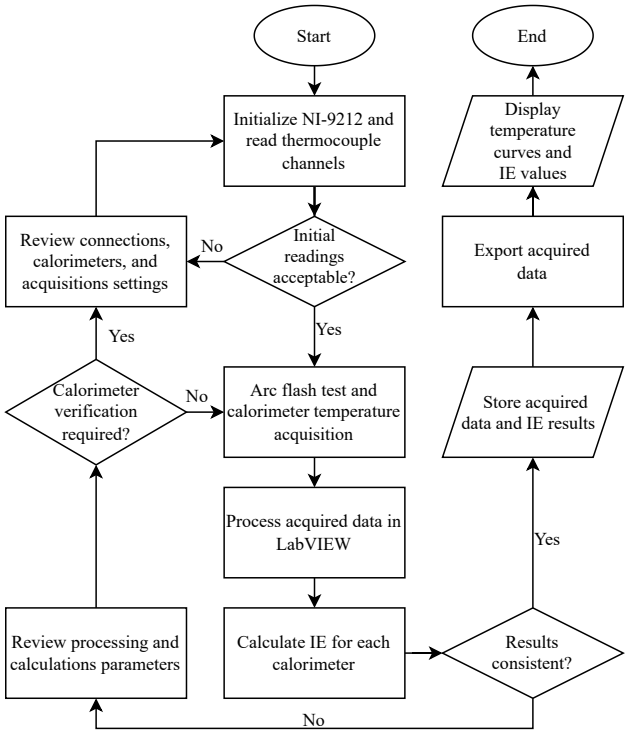


FIGURE 6. LabVIEW-based acquisition and processing workflow.

the user or an error condition is detected. This integration reduces the reliance on non-integrated post-processing and provides a consistent data flow from signal acquisition to result storage.

B. Incident Energy Calculation and Data Management

For each calorimeter, the processing routine determines the initial temperature, T_0, as the mean temperature over the stable pre-arc interval, and the maximum temperature, $T_{\max}$, reached after arc extinction. These values define the temperature interval used to calculate the enthalpy change of the copper disk.

The temperature-dependent molar heat capacity of solid copper is represented by the Shomate equation:

$$C_p(t) = A + B \cdot t + C \cdot t^2 + D \cdot t^3 + \frac{E}{t^2}, \tag{1}$$

where $t = T/1000$, with T expressed in kelvin, and $C_p(t)$ is expressed in J/(mol·K). The Shomate coefficients used in (1) are provided in the footnote.[1] After converting T_0 and $T_{\max}$ to kelvin, the scaled temperatures are $t_0 = T_0/1000$ and $t_{\max} = T_{\max}/1000$, and the IE (cal/cm^2) is given by

$$IE = \frac{1000 \cdot m}{4.184 \cdot a \cdot M_{\mathrm{Cu}}} \int_{t_0}^{t_{\max}} C_p(t)\, dt, \tag{2}$$

where m is the copper-disk mass in grams, a is its exposed surface area in cm^2, and $M_{\mathrm{Cu}} = 63.546$ g/mol is the molar mass of copper. The factor 4.184 converts joules to calories, whereas the factor 1000 results from the scaled-temperature definition, since $dT = 1000 \cdot dt$.

Substituting (1) into (2) and analytically evaluating the integral yields

$$IE = \frac{1000 \cdot m}{a \cdot M_{\mathrm{Cu}} \cdot 4.184} \left[A \cdot (t_{\max} - t_0) + B \cdot \left(\frac{t_{\max}^2 - t_0^2}{2} \right) + C \cdot \left(\frac{t_{\max}^3 - t_0^3}{3} \right) + D \cdot \left(\frac{t_{\max}^4 - t_0^4}{4} \right) + E \cdot \left(\frac{1}{t_0} - \frac{1}{t_{\max}} \right) \right]. \tag{3}$$

The VI applies (3) to the thermal parameters identified from each recorded curve and automatically calculates the IE. The temperature-time curve defines the integration limits, while the absorbed energy is obtained from the enthalpy change over the corresponding scaled temperature interval, from t_0 to $t_{\max}$.

For each test, the highest IE measured among the seven calorimeters was adopted as the experimental value for comparison with the corresponding IEEE Std 1584-2018 estimate. This criterion represents the position subjected to the greatest measured thermal exposure and maintains consistency with the calorimetric procedure adopted in the development of the IEEE Std 1584-2018 IE model [3], [24].

[1] Shomate coefficients for solid copper between 298 and 1358 K: $A = 17.72891$, $B = 28.09870$, $C = -31.25289$, $D = 13.97243$, and $E = 0.068611$ [14].

The developed virtual instrument provides real-time monitoring of the temperature curves, allowing the user to inspect signal continuity and identify possible anomalous measurements before the results are stored. Upon completion of the test, the VI automatically identifies the initial and maximum temperatures, calculates the IE values using (2), and displays the numerical results. Finally, the temperature arrays, identified thermal parameters, and calculated IE values are exported to structured files, ensuring data traceability without the need for non-integrated post-processing.

After each test, the VI stores the temperature curves, identified thermal parameters, and calculated IE values in structured files. This procedure facilitates data retrieval and comparison with a separately implemented reference calculation and the IEEE Std 1584-2018 calculations.

III. EXPERIMENTAL RESULTS

This section presents and discusses the performance of the proposed thermocouple-based IE measurement system. The analysis begins with the functional verification of the seven calorimeters and the characterization of the electrical and thermal conditions of the arc flash tests. The measured IE values and the numerical consistency of the automated calculation are then evaluated. Finally, the experimental measurements are compared with the corresponding values calculated according to IEEE Std 1584-2018.

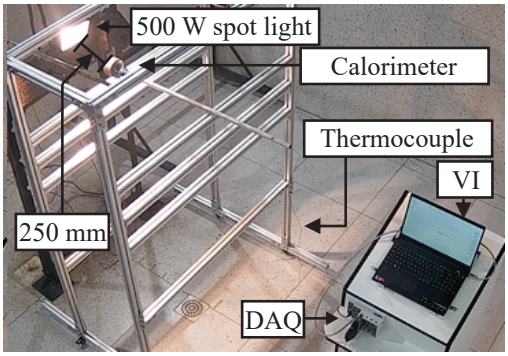
A. Calorimeter Verification by Spotlight Exposure

Before the arc flash tests, the seven calorimeters and acquisition channels underwent functional verification according to IEC 61482-1-1 [7]. The procedure was not used for calibration, and no correction or adjustment was applied based on its results. Each calorimeter was individually exposed for 30 s to a 500 W spotlight at 250 mm. The beam was centered on and perpendicular to the exposed surface.

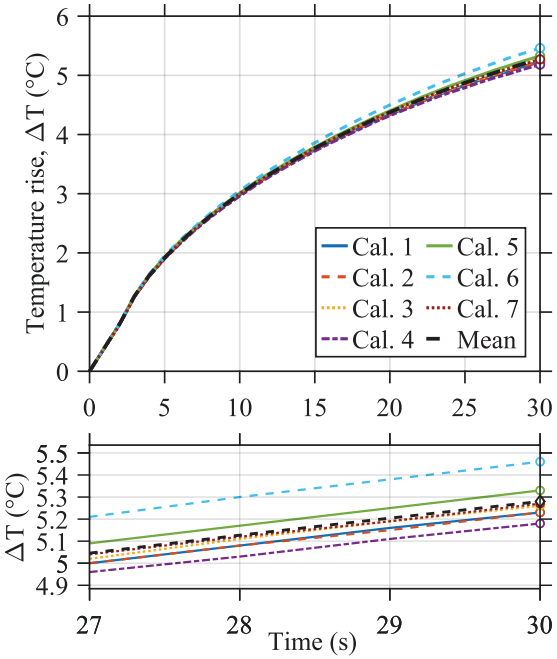
The temperature recorded immediately before the spotlight was energized was adopted as the initial temperature, T_0, for each calorimeter. Before each exposure, the initial temperatures were monitored to avoid thermal interference from preceding measurements. The temperature response was then recorded throughout the exposure using the developed acquisition system. The experimental arrangement and the corresponding temperature-rise curves are shown in Fig. 7.

As shown in Fig. 7b, all calorimeters exhibited smooth and monotonic temperature increases throughout the 30 s exposure, with closely grouped responses and similar heating profiles. The dashed curve represents the mean temperature rise, while the enlarged view of the final 3 s highlights the small differences among the individual responses.

The initial temperatures ranged from 21.33 to 23.03 °C, corresponding to a maximum spread of 1.70 °C and satisfying the initial-temperature condition specified for the verification procedure. At 30 s, the temperature rises ranged from 5.18 to 5.46 °C, with a mean of 5.28 °C.



(a)



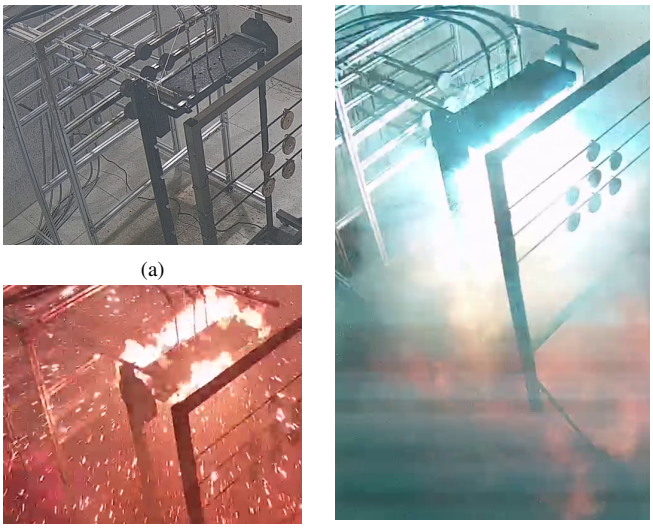
(b)

FIGURE 7. Spotlight-based functional verification of the calorimeters: (a) experimental arrangement and (b) temperature elevation curves recorded during the 30 s exposures.

The maximum absolute deviation from the mean response at 30 s was 0.18 °C, observed for calorimeter 6. This value was well below the maximum deviation of 4 °C specified in IEC 61482-1-1 [7]. Therefore, all seven calorimeters satisfied the functional-verification criterion and exhibited consistent thermal responses under the test conditions.

B. Selected Arc Flash Test IE Determination

A selected test was used to describe the electrical-data processing and IE measurement procedure. The test was performed in the VOA configuration at a V_{oc} of 1.1 kV, with a 100 mm electrode gap and a 500 mm working distance. The ambient temperature and relative humidity during the test were 17.9 °C and 90%, respectively. The evolution of the arc from inception to extinction is shown in Fig. 8.



(a) (c) (b)

FIGURE 8. Arc evolution during the selected test in the VOA configuration: (a) inception, (b) developed arc showing its spatial extension, and (c) extinction.

The three-phase current signals were obtained from oscillographic records generated by three protection relays and exported in COMTRADE format. The corresponding `.dat` and `.cfg` files were imported into MATLAB®, where the signals were converted to primary-current values using the appropriate scaling factors.

The current samples were processed using an adapted cosine-filter implementation based on Annex G of IEEE Std 1584-2018 [3]. The filter was used to extract the fundamental current component while attenuating the decaying dc component and higher-order harmonics.

The number of samples per cycle, N_s, was determined from the recording sampling rate and the 60 Hz fundamental frequency. The normalization and indexing of the cosine filter were adapted to the sampling structure of the recorded signals. The cosine-filter coefficients were calculated as

$$CFC_k = \cos\left(\frac{2\pi k}{N_s}\right), \qquad k = 1, \ldots, N_s. \tag{4}$$

For each phase, the filtered-current sequence was obtained over a one-cycle moving window according to

$$i_{f,p}(m) = \frac{2}{N_s}\sum_{k=1}^{N_s} i_p(m-k)\, CFC_k, \qquad p = A, B, C. \tag{5}$$

where $i_p(m-k)$ represents the measured current samples of phase p, $i_{f,p}(m)$ is the corresponding cosine-filter output, and m identifies the position of the moving window along the recorded signal.

Annex G obtains the fundamental-component magnitude from the cosine-filter output and a corresponding output displaced by one quarter of a cycle. In the adopted implementation, the rms current was instead calculated directly from the retained filtered-current sequence:

$$I_p = \sqrt{\frac{1}{N_R}\sum_{m=1}^{N_R} i_{f,p}^2(m)}, \qquad p = A, B, C. \tag{6}$$

where N_R is the number of filtered-current samples retained after excluding the first two cycles from the rms-current calculation. The resulting rms values of phases A, B, and C were averaged to determine the arcing current, I_{arc}.

The arc duration, t_{arc}, was determined from the unfiltered three-phase current records using a threshold equal to 10% of a reference current. This reference was defined as the maximum combined instantaneous magnitude of the three-phase currents after the first two cycles of the initially detected event, to reduce the influence of the initial arc-establishment transient on the threshold definition. Arc ignition and extinction corresponded to the first and last samples, respectively, exceeding this threshold in the complete current record. Thus, the first two cycles were retained in t_{arc} and excluded only from the determination of the reference current and from the rms-current calculation. The resulting arcing currents and arc duration are summarized in Table 1.

The phase rms currents were 5.409, 5.755, and 4.997 kA for phases A, B, and C, respectively, resulting in a mean I_{arc} of 5.387 kA. The arc duration used in the IEEE Std 1584-2018 IE calculation was 485 ms, corresponding to the interval from arc ignition to extinction. At 60 Hz, the two excluded cycles correspond to 33.333 ms; however, this exclusion was applied only to the reference-current determination and the rms-current calculation and did not reduce t_{arc} used in the IEEE Std 1584-2018 calculation.

Figure 9 shows the temperature records of the seven calorimeters during the selected test. The temperatures remained stable before arc ignition and then increased due to the thermal exposure. No evident EMI-related disturbances requiring additional signal processing were observed in the thermocouple signals during the arc event.

For each calorimeter, the initial temperature, T_0, was determined as the mean temperature over the stable pre-arc interval, whereas $T_{\max}$ was defined as the maximum temperature reached after arc extinction. The corresponding temperature rise was calculated as $\Delta T = T_{\max} - T_0$. These thermal parameters and the IE values calculated by the VI are summarized in Table 2.

The measured IE ranged from 1.33 to 3.12 cal/cm^2, with a mean of 2.46 cal/cm^2. The highest value was recorded by the central calorimeter, aligned with the electrode tips,

TABLE 1. Arcing Currents and Duration for the Selected Test

Parameter	Value
Phase-A filtered rms current, I_A	5.409 kA
Phase-B filtered rms current, I_B	5.755 kA
Phase-C filtered rms current, I_C	4.997 kA
Mean arcing current, I_{arc}	5.387 kA
Arc duration, t_{arc}	485 ms

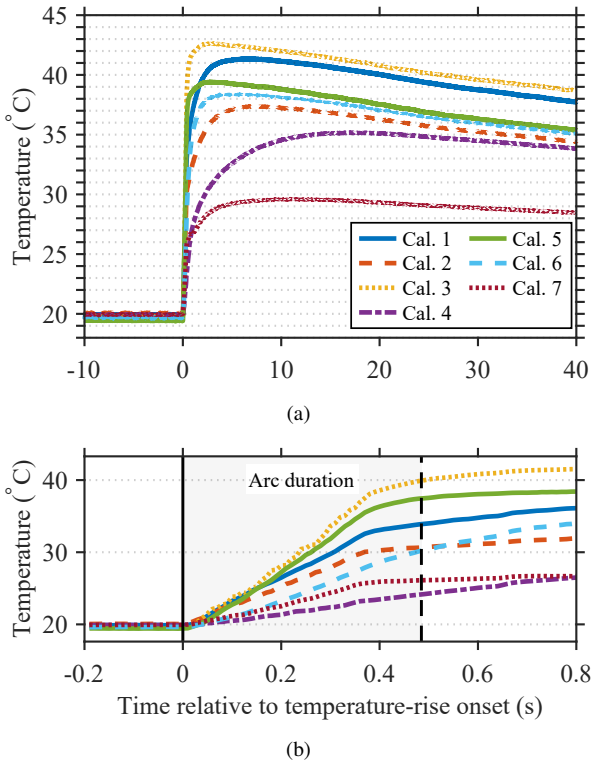


FIGURE 9. Temperature rise of the seven calorimeters: (a) complete response and (b) enlarged view during the arc interval.

TABLE 2. Calorimetric results for the selected test.

Position	Mass (g)	T_0 (°C)	$T_{\max}$ (°C)	ΔT (°C)	IE (cal/cm^2)
1	18.8584	19.572	41.390	21.818	2.97
2	18.8482	20.004	37.397	17.393	2.39
3	18.6092	19.838	42.658	22.820	3.12
4	18.8523	19.853	35.187	15.334	2.11
5	18.9418	19.140	39.432	20.292	2.79
6	18.3751	19.559	38.420	18.861	2.50
7	18.7814	19.890	29.631	9.741	1.33
Mean	**18.7523**	**19.694**	**37.731**	**18.037**	**2.46**

whereas the lowest occurred at position 7. Despite its lower magnitude, the thermal response at position 7 exhibited the same general heating and cooling behavior as the other calorimeters, and this sensor had previously satisfied the spotlight-based functional-verification criterion. The value was therefore retained, although the origin of this local reduction could not be established.

The enlarged view in Fig. 9b provides greater detail of the initial thermal response during the arc interval. The calorimeter temperatures increase progressively over this short period, with different heating rates among the measurement positions. The temperature continues to evolve after the arc interval, consistent with the thermal inertia of the copper calorimeters and the redistribution of absorbed heat.

Accordingly, the maximum among the seven calorimeters was adopted as the experimental IE for comparison with the IEEE Std 1584-2018 estimate [3], [24]. This maximum was recorded by calorimeter 3, whose VI calculation was nu-

CC BY

merically verified using $m_3 = 18.6092$ g, $a = 12.566$ cm^2, $t_0 = 0.292988$, and $t_{\max} = 0.315808$. Evaluation of the integral in (2) yielded 0.55957, corresponding to a molar enthalpy change of 0.55957 kJ/mol. Substitution into (2) gives

$$IE_3 = \frac{1000 \cdot 18.6092 \cdot 0.55957}{12.566 \cdot 63.546 \cdot 4.184} \approx 3.12 \text{ cal/cm}^2. \quad (7)$$

The LabVIEW VI also yielded an IE of 3.12 cal/cm^2, matching the analytical result at the adopted precision of two decimal places and confirming numerical agreement between the two calculations.

Figure 10 presents the input parameters and the corresponding IEEE Std 1584-2018 IE estimate for the selected VOA test. The previously specified electrical and geometric parameters, together with the processed $I_{\text{arc}} = 5.387$ kA and $t_{\text{arc}} = 485$ ms, were entered into the publicly accessible IEEE DataPort™ arc flash IE and arcing current calculator [3], [25]. Since the complete IEEE Std 1584-2018 calculation procedure involves multiple equations, configuration-dependent coefficients, and intermediate calculation steps, its full reproduction would be disproportionate to the scope of this work. The open-access IEEE DataPort tool provides a public implementation of the calculation procedure, allowing the adopted calculation to be reproduced without requiring direct access to the complete standard. The calculation was also independently reproduced using an adapted spreadsheet based on the mathematical formulation of the standard.

The maximum experimental IE measured by the calorimeter array was 3.12 cal/cm^2, whereas the IEEE Std 1584-2018 calculation yielded 4.41 cal/cm^2. The experimental value was therefore 1.29 cal/cm^2, or approximately 29.3%, lower than the IEEE-based estimate. Thus, under the investigated VOA conditions, the empirical model yielded a higher IE estimate than the calorimetric measurement.

The observed difference may reflect the actual arc trajectory, the spatial distribution of the thermal exposure, and the empirical nature of the IEEE Std 1584-2018 model. The experimental result corresponds to the highest IE measured among the seven discrete calorimeter positions, whereas the IEEE calculation provides an empirical estimate for the specified electrical and geometric conditions. For this individual test, the observed difference should not be generalized to other test conditions.

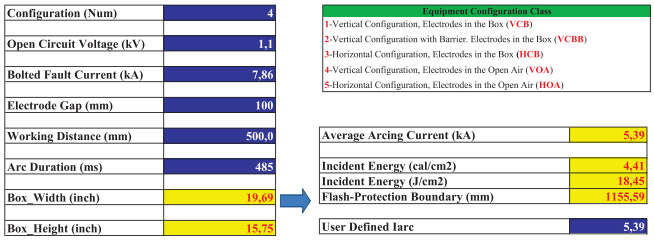


FIGURE 10. IEEE Std 1584-2018 input parameters and resulting IE estimate for the selected VOA test [25].

C. Comparative Analysis with IEEE Std 1584-2018

To provide a broader assessment beyond the selected test, the maximum IE measured by the calorimeter array was compared with the corresponding IEEE Std 1584-2018 estimate for the investigated HOA and VOA tests. The experimental campaign covered different electrical and geometric conditions, including current levels, arc durations, and working distances. Therefore, the comparison presented here provides an overall view of the agreement between the calorimetric measurements and the empirical model across the investigated conditions, rather than a direct comparison between HOA and VOA under identical test conditions.

The IEEE Std 1584-2018 estimates were obtained using IEEE DataPort [25], with the electrical and geometric parameters determined for each test. The relative difference was calculated with respect to the IEEE Std 1584-2018 estimate, with negative values indicating measured IE below the corresponding IEEE estimate. Figure 11 summarizes the results for the 18 tests included in the comparison, comprising 10 VOA and 8 HOA tests.

The measured IE remained below the corresponding IEEE Std 1584-2018 estimate in all evaluated cases, with relative differences ranging from approximately -29.3% to -2.6%. The overall mean relative difference was approximately -12.7%, showing that the magnitude of the difference varied among the investigated conditions rather than being constant.

When the results are examined separately, the VOA tests exhibited relative differences ranging from approximately

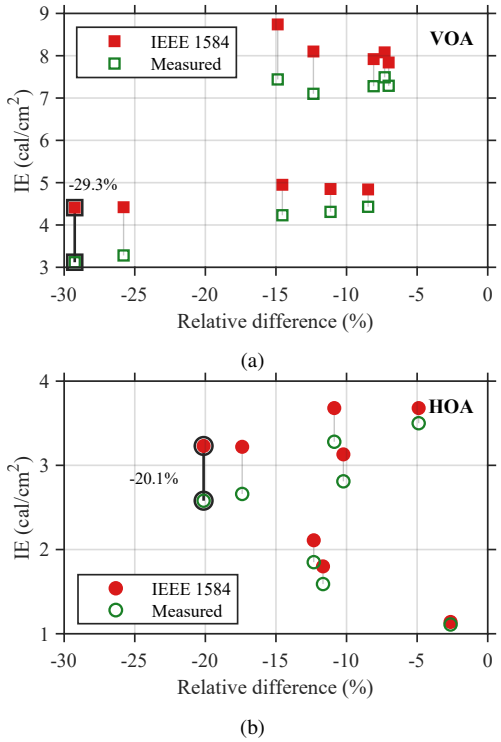


FIGURE 11. Comparison between experimentally measured IE and IEEE Std 1584-2018 estimates plotted as a function of the relative difference for: (a) VOA configuration and (b) HOA configuration.

-29.3% to -7.0%, with a mean of -13.9%, whereas the HOA tests ranged from approximately -20.1% to -2.6%, with a mean of -11.3%.

For the VOA configuration, the largest relative difference was approximately -29.3%, corresponding to the selected test analyzed in detail in the preceding section and previously reported in [16]. In this test, the seven calorimeters measured incident-energy values ranging from 1.33 to 3.12 cal/cm^2, indicating pronounced spatial variation of the thermal exposure. The developed arc also exhibited significant spatial extension. Since the experimental value corresponds to the maximum IE measured at discrete calorimeter positions, the arc trajectory and resulting spatial distribution may have contributed to the observed difference. The second largest VOA difference was approximately -25.8%, while tests with higher predicted IE levels generally exhibited smaller relative differences. Therefore, the deviation cannot be explained solely by the IE level.

For the HOA configuration, the largest relative difference was approximately -20.1%, followed by a second difference of approximately -17.4%. Both tests were performed at a working distance of 800 mm, with measured IE values of 2.58 and 2.66 cal/cm^2 and IEEE Std 1584-2018 estimates of 3.23 and 3.22 cal/cm^2, respectively. However, other HOA tests performed at the same working distance exhibited smaller relative differences. Thus, working distance alone does not explain the larger deviations, while the similarity between these two cases indicates that the most divergent HOA result was not an isolated measurement.

Overall, the analysis of the most divergent cases indicates that the observed differences cannot be associated with a single experimental parameter. They may instead reflect the combined influence of arc behavior, spatial thermal distribution, calorimeter position, and the electrical and geometric conditions of each test. Since these effects were not independently isolated, the results should be interpreted as a characterization of the agreement obtained under the investigated conditions rather than as evidence of a systematic bias of IEEE Std 1584-2018.

IV. CONCLUSION

The results obtained in this study indicate that thermocouple-based copper calorimetry can be integrated with isolated data acquisition and VI for IE determination in arc flash tests. The developed architecture combined temperature acquisition, thermal-parameter identification, Shomate-based enthalpy calculations, visualization, and data storage within a single processing workflow.

The experimental evaluation addressed complementary stages of the measurement chain. The seven calorimeters satisfied the functional-verification criterion of IEC 61482-1-1, while the detailed VOA test allowed the complete procedure from electrical-data processing to calorimetric IE determination to be examined. Across the expanded set of 18 HOA and VOA tests, the measured IE values remained consistently below the corresponding IEEE Std 1584-2018 estimates, although the magnitude of the relative difference varied among the investigated conditions.

The main contribution of this work lies in the integration and experimental evaluation of the calorimetric measurement chain as a unified acquisition and processing system. The comparison with IEEE Std 1584-2018 is therefore treated as a complementary reference for interpreting the experimental results, rather than as an evaluation or proposed modification of the empirical model. The expanded experimental set also provides a broader context for the detailed test previously reported in the conference study. Although this selected case presented the largest relative difference from the IEEE Std 1584-2018 estimate, the remaining tests exhibited different levels of agreement, indicating that the relationship between measured and IEEE-based IE should be examined across multiple test conditions rather than inferred from an individual arc flash event.

From an experimental perspective, the proposed architecture provides a structured procedure for acquiring, processing, reviewing, and storing calorimetric IE data in high-current laboratory tests. The consistent ordering observed in the investigated data set, with measured IE below the corresponding IEEE estimates, should nevertheless be interpreted within the specific electrical and geometric conditions of the experiments. Calorimetric measurements represent the thermal exposure at discrete experimental positions, whereas IEEE Std 1584-2018 provides an empirical estimate for the specified test conditions; consequently, the observed differences should not be interpreted as a fixed relationship between the two approaches.

The conclusions of this study apply to the investigated experimental conditions, which included different electrical and geometric parameters and discrete calorimeter positions. Within this scope, the developed system provided a consistent framework for IE acquisition, processing, and comparison across the evaluated arc flash tests. The same framework can be extended to other test conditions and experimental arrangements to further characterize the influence of arc behavior and measurement position on the spatial distribution of IE.

ACKNOWLEDGMENT

The authors would like to thank the CPFL group for technical and financial support, through the Research, Development and Innovation project PD-00063-3104/2024 with resources from PDI ANEEL program. This study was financed in part by the Coordenação de Aperfeiçoamento de Pessoal de Nível Superior – Brasil (CAPES/PROEX) – Finance Code 001. They also acknowledge the Federal University of Santa Maria (UFSM), the Graduate Program in Electrical Engineering (PPGEE-UFSM), and the Institute of Energy and Mobility (IEM) for their institutional support and for providing the academic and laboratory infrastructure essential to this work.

CC BY

AUTHOR'S CONTRIBUTIONS

A.A.S.PEREIRA: Conceptualization, Data Curation, Formal Analysis, Investigation, Methodology, Software, Validation, Visualization, Writing – Original Draft, and Writing – Review & Editing. **P.O.BACIN:** Conceptualization, Data Curation, Formal Analysis, Funding Acquisition, Investigation, Methodology, Supervision, Validation, Visualization, Writing – Original Draft, and Writing – Review & Editing. **V.C.BENDER:** Conceptualization, Methodology, Funding Acquisition, Project Administration, Resources, Supervision, and Writing – Review & Editing. **M.BOTTARO:** Conceptualization, Data Curation, Methodology, Software, Supervision, Validation, and Writing – Review & Editing. **T.B.MARCHESAN:** Conceptualization, Funding Acquisition, Resources, and Writing – Review & Editing. **G.J.G.SANTOS:** Funding Acquisition, Resources, Supervision, and Writing – Review & Editing. **J.P.BEGOSSI:** Project Administration, Resources, and Writing – Review & Editing.

PLAGIARISM POLICY

This article was submitted to the similarity system provided by Crossref and powered by iThenticate – Similarity Check.

DATA AVAILABILITY

The data used in this research is available in the body of the document.

REFERENCES

[1] A. D. Stokes and W. T. Oppenlander, "Electric Arcs in Open Air," *Journal of Physics D: Applied Physics*, vol. 24, no. 1, pp. 26–35, 1991, doi: 10.1088/0022-3727/24/1/006.

[2] R. H. Lee, "The Other Electrical Hazard: Electric Arc Blast Burns," *IEEE Transactions on Industry Applications*, vol. IA-18, no. 3, pp. 246–251, 1982, doi: 10.1109/TIA.1982.4504068.

[3] *IEEE Guide for Performing Arc-Flash Hazard Calculations*, IEEE Std 1584-2018 (Revision of IEEE Std 1584-2002). Piscataway, NJ, USA: IEEE, Nov. 2018, pp. 1–134, doi: 10.1109/IEEESTD.2018.8563139.

[4] NFPA, *NFPA 70E: Standard for Electrical Safety in the Workplace*, 2027 ed. Quincy, MA, USA: National Fire Protection Association, 2026.

[5] Brazil, Ministry of Labor and Employment, "Portaria MTE No. 737, de 29 de maio de 2026: Aprova a nova redação da Norma Regulamentadora No. 10 (NR-10)—Segurança em Instalações Elétricas e Serviços em Eletricidade," *Diário Oficial da União*, ed. 101, sec. 1, p. 167, Jun. 1, 2026.

[6] ASTM International, *ASTM F1959/F1959M-24b: Standard Test Method for Determining the Arc Rating of Materials for Clothing*. West Conshohocken, PA, USA: ASTM International, 2024.

[7] IEC 61482-1-1, *Live Working—Protective Clothing Against the Thermal Hazards of an Electric Arc—Part 1-1: Test Methods—Method 1: Determination of the Arc Rating (ELIM, ATPV and/or EBT50) of Clothing Materials and Protective Clothing Using an Open Arc*, IEC Standard 61482-1-1, Edition 2.0, Geneva, Switzerland, 2019.

[8] P. O. Bacin et al., "Infrared Thermography for Incident Energy Measurement in Arc Flashes under VOA Configuration Supported by Statistical Analysis," in *2025 IEEE ESW Brazil – Electrical Safety Workshop Brazil (ESW Brazil)*, São Paulo, Brazil, 2025, pp. 1–8, doi: 10.1109/ESWBrazil64921.2025.11277734.

[9] M. Bottaro, L. E. Caires, P. F. Obase, T. O. de Carvalho, and H. Tatizawa, "A Comprehensive Analysis of the Influence of Thermal Insulating Materials on Arc Rating Tests," *IEEE Transactions on Instrumentation and Measurement*, vol. 74, Art. no. 1500609, pp. 1–9, 2025, doi: 10.1109/TIM.2025.3529562.

[10] ASTM Committee E20 on Temperature Measurement, *Manual on the Use of Thermocouples in Temperature Measurement*, R. M. Park, Ed., 4th ed., ASTM MNL12, Revision of ASTM STP 470B. West Conshohocken, PA, USA: ASTM International, 1993, doi: 10.1520/MNL12-4TH-EB.

[11] N. Henderson, "Practical Temperature Measurements," Application Note, VTI Instruments, AMETEK Programmable Power, San Diego, CA, USA. [Online]. Available: https://www.vtiinstruments.com/knowledge-center/white-papers

[12] Z. Zhang, W.-J. Lee, and D. A. Dini, "Grounding and Isolation of Sensitive Measurement Equipment for Arc Flash Testing at High-Power Laboratory," *IEEE Transactions on Industry Applications*, vol. 51, no. 6, pp. 5281–5287, Nov./Dec. 2015, doi: 10.1109/TIA.2015.2411654.

[13] F. C. S. Soares et al., "Measurement of Arc Flash Incident Energy in Low-Voltage Three-Phase Panels Using an Optical Calorimeter," in *2025 IEEE ESW Brazil – Electrical Safety Workshop Brazil (ESW Brazil)*, São Paulo, Brazil, 2025, pp. 1–5, doi: 10.1109/ESWBrazil64921.2025.11277722.

[14] M. W. Chase, Jr., *NIST-JANAF Thermochemical Tables*, 4th ed., J. Phys. Chem. Ref. Data, Monograph No. 9. Washington, DC, USA: American Chemical Society, 1998. ISBN: 978-1-56396-831-0.

[15] M. Bottaro, *Instrumentação Virtual em Laboratório: Introdução ao LabVIEW*, São Paulo, Brasil: Instituto de Eletrotécnica e Energia da Universidade de São Paulo (IEE-USP), 2012, 125 p., ISBN: 978-85-86923-27-2.

[16] A. A. S. Pereira et al., "Metodologia de Instrumentação e Medição da Energia Incidente de Arcos Elétricos por Termopares," in *Proceedings of the 17th Seminar on Power Electronics and Control (SEPOC 2025)*, 2025, doi: 10.53316/sepoc2025.002.

[17] P. O. Bacin et al., "Incident Energy Determination of Three-Phase Arc Flash Using Magnetohydrodynamics Simulations: A Case Study for Horizontal Electrodes in Open-Air Configurations," *High Voltage*, vol. 10, no. 2, pp. 436–450, 2025, doi: 10.1049/hve2.70009.

[18] F. C. S. Soares et al., "Development of an Optical Calorimeter Sensor for the Arc Thermal Performance Value (ATPV) Determination on Arc-Rated Materials for Personal Protective Equipment," *Sensors*, vol. 26, no. 8, p. 2352, 2026, doi: 10.3390/s26082352.

[19] P. O. Bacin, "Contribuição ao desenvolvimento de um laboratório de arcos elétricos para a medição da energia incidente," M.S. thesis, Graduate Program in Electrical Engineering, Federal University of Santa Maria, Santa Maria, RS, Brazil, 2022. URL: https://repositorio.ufsm.br/handle/1/26218.

[20] C. S. Mardegan, F. B. Resende, and M. Bottaro, *Arco Elétrico e Energia Incidente: Metodologias de Cálculo em Sistemas AC e DC, EPIs, EPCs, Técnicas para Redução da EI e Equipamentos e Dispositivos para Melhorar a Segurança*. 1st ed. São Paulo, SP, Brasil: Ed. do Autor, 2025, ISBN: 978-65-01-41915-2.

[21] L. M. R. Baccarini, B. R. de Menezes, L. H. Batista, and W. M. Caminhas, "Identificação de Falhas Utilizando Informações de Sensores Presentes no Quadro de Comando dos Motores," *Eletrônica de Potência*, vol. 17, no. 4, pp. 763–770, Nov. 2012, doi: 10.18618/REP.2012.4.763770.

[22] S. A. O. da Silva, D. H. Wollz, and L. P. Sampaio, "Development of a Didactic Workbench Using Real-Time Monitoring System for Teaching of Photovoltaic Systems," *Eletrônica de Potência*, vol. 23, no. 3, pp. 371–381, Sep. 2018, doi: 10.18618/REP.2018.3.2793.

[23] National Instruments, *LabVIEW*, Austin, TX, USA. [Online]. Available: https://www.ni.com/labview

[24] W.-J. Lee, T. L. Gammon, and Z. Zhang, "Systems and Methods for Arc Flash Hazard Assessment," U.S. Patent 9,146,267 B2, Sep. 29, 2015.

[25] IEEE Standards Association, "Arc Flash IE and Iarc Calculators," IEEE DataPort Dataset, Dec. 19, 2019, doi: 10.21227/8gch-a963.

BIOGRAPHIES

Andrey A. S. Pereira was born in Santa Maria, Brazil, in 1999. He is currently pursuing the B.S. degree in Telecommunications Engineering at the Federal University of Santa Maria (UFSM), Santa Maria, Brazil. From 2024 to 2026, he served as an undergraduate researcher at the High-Current Laboratory (HCLab) of the Institute of Energy and Mobility

(IEM) at UFSM, contributing to the development of automated measurement instrumentation and calorimetric algorithms for arc-flash evaluation. Since January 2026, he has been an Engineering Intern at Embraer Radares in Campinas, Brazil, working on defense radar systems. His research interests include arc-flash testing, incident energy assessment, virtual instrumentation, calorimetry, and radar systems.

Pedro O. Bacin was born in Jaguari, Brazil, in 1996. He received the B.S. and M.S. degrees in electrical engineering from the Federal University of Santa Maria (UFSM), Santa Maria, Brazil, in 2020 and 2022, respectively. He also completed a postgraduate specialization in Occupational Safety Engineering at Cruzeiro do Sul University, São Paulo, Brazil, in 2021, and received a teaching degree in Industrial Control and Processes from UFSM in 2022. He is currently a Ph.D. candidate in electrical engineering at UFSM. From 2022 to 2025, he served as the Technical Manager of the High-Current Laboratory (HCLab) at the Institute of Energy and Mobility (IEM) of UFSM. Since 2025, he has been an Electricity Teacher at the Municipal School of Industrial Apprenticeship (EMAI), Santa Maria, Brazil. His research interests include arc-flash testing, incident energy assessment, infrared thermography, calorimetry, and electrical safety.

Vitor C. Bender was born in Panambi, Brazil, in 1987. He received the B.S. degree in Electrical Engineering from the Regional University of Northwestern Rio Grande do Sul (UNIJUÍ), Brazil, in 2011, and the M.S. and Ph.D. degrees in Electrical Engineering from the Federal University of Santa Maria (UFSM), Santa Maria, Brazil, in 2012 and 2015, respectively. In 2014, he was a visiting researcher at the University of Oviedo, Spain. From 2015 to 2017, he was a Professor at the Federal University of Pampa (UNIPAMPA). Since 2018, he has been an Adjunct Professor at UFSM, where he currently serves as Director of the Institute of Energy and Mobility (IEM) and permanent faculty member of the Graduate Program in Electrical Engineering. He is a CNPq DT-2 Productivity Fellow, IEEE Senior Member, and CIGRE member. His research interests include electrical arcs, incident energy, high-voltage equipment, thermal modeling, and computer-aided engineering.

Marcio Bottaro received the B.S. degree in Electronic Technology in 1995, and the M.S. and Ph.D. degrees in Nuclear Technology Applications in 2007 and 2012, respectively. He currently serves as Technical Supervisor of the Electrical Equipment and Materials Safety Section at the Institute of Energy and Environment of the University of São Paulo (IEE-USP), São Paulo, Brazil. Previously, he was the Technical Manager of the Brazilian Arc Flash Laboratory Project, a partnership between USP and Petrobras, the first standard open-arc laboratory in the Southern Hemisphere. Since 2018, he has served as the convenor of the Thermal Risks Studies Commission of the Brazilian National Committee ABNT/CB-32, acting as a Brazilian Specialist in IEC TC 78 (Live Working) and IEC TC 128 (Operation of Electrical Installations). His research interests include safety of electrical equipment and materials, electrical and thermal testing of personal protective equipment (PPE), and type testing of medical electrical equipment.

Tiago B. Marchesan was born in Santa Maria, Brazil, in 1980. He received the B.S. (Hons.) and Ph.D. degrees in electrical engineering from the Federal University of Santa Maria (UFSM), Santa Maria, Brazil, in 2003 and 2008, respectively. From 2009 to 2011, he worked as a Research and Development Engineer with the Power Transformer Group at WEG Electric Corporation, Jaraguá do Sul, Brazil, and as a Professor at the University of Vale do Rio dos Sinos (UNISINOS), São Leopoldo, Brazil. Since 2011, he has been a Professor at UFSM, where he served as Director of the Technology Center from 2018 to 2025. Since 2026, he has served as Vice President of UFSM. He is also involved in industry-oriented research and development projects. His research interests include smart grids, power transformers, and electric power systems.

Gilnei J. G. dos Santos was born in Camaquã, Brazil, in 1976. He received the B.S. degree in Electrical Engineering from the Lutheran University of Brazil (ULBRA), Canoas, Brazil, in 2009, and a postgraduate degree in Occupational Safety Engineering from the same institution in 2013. He earned an MBA in Project Management from the University of Vale do Rio dos Sinos (UNISINOS), São Leopoldo, Brazil, in 2017, and the M.S. degree in Electrical Engineering from the Federal University of Santa Maria (UFSM), Santa Maria, Brazil, in 2020. He is currently pursuing the Ph.D. degree in Electrical Engineering at UFSM. He currently works as a Specialist Engineer at CPFL Energia, focusing on technical standards, equipment specification, operational process management, and R&D projects for the electric power sector. His research interests include arc-flash testing, incident energy assessment, electrical safety, infrared thermography, and calorimetric methods.

Jéssica P. Begossi was born in Campinas, Brazil, in 1991. She received the B.S. and teaching degrees in Environmental Studies from the University of Campinas (UNICAMP), Campinas, Brazil, in 2013, and the B.S. degree in Environmental and Sanitary Engineering from the Pontifical Catholic University of Campinas (PUC-Campinas), Campinas, Brazil, in 2018. She also completed an MBA in Project Management from the University of São Paulo (USP/ESALQ), Piracicaba, Brazil, in 2026. From 2017 to 2022, she worked as an R&D Analyst in the electric power sector at Neoenergia Elektro. Since 2023, she has been an Innovation Analyst for R&D projects at CPFL Energia, Campinas, Brazil. Her research interests include electrical engineering, electrical safety, incident energy assessment, and power sector innovation.

CC BY